ACS Catalysis

Research Article

pubs.acs.org/acscatalysis

Efficient Polymerization of the Aniline Dimer *p*-Aminodiphenylamine (PADPA) with *Trametes versicolor* Laccase/O_2 as Catalyst and Oxidant and AOT Vesicles as Templates

Katja Junker,[†] Sandra Luginbühl,[†] Mischa Schüttel,[†] Louis Bertschi,[‡] Reinhard Kissner,[§] Lukas D. Schuler,[⊥] Boris Rakvin,[¶] and Peter Walde*[,†]

[†]Laboratory of Polymer Chemistry, Department of Materials, ETH Zürich, Vladimir-Prelog-Weg 5, CH-8093 Zürich, Switzerland

[‡]Mass Spectrometry Service Facility, Laboratory of Organic Chemistry, Department of Chemistry and Applied Biosciences, Vladimir-Prelog-Weg 3, CH-8093 Zürich, Switzerland

[§]Laboratory of Inorganic Chemistry, Department of Chemistry and Applied Biosciences, Vladimir-Prelog-Weg 2, CH-8093 Zürich, Switzerland

[⊥]xirrus GmbH, Buchzelgstrasse 36, CH-8053 Zürich, Switzerland

[¶]Division of Physical Chemistry, Ruđer Bošković Institute, Bijenička c. 54, HR-10002 Zagreb, Croatia

Supporting Information

ABSTRACT: The aniline dimer PADPA (= *p*-aminodiphenylamine = *N*-phenyl-1,4-phenylenediamine) was polymerized to poly(PADPA) at 25 °C with *Trametes versicolor* laccase (TvL)/O_2 as catalyst and oxidant and in the presence of vesicles formed from sodium bis(2-ethylhexyl) sulfosuccinate (AOT) as templates. In comparison to the previously studied polymerization of aniline with the same type of enzyme−vesicle system, the polymerization of PADPA is much faster, and considerably fewer enzymes are required for complete monomer conversion. Turbidity measurements indicate that PADPA strongly binds to the vesicle surface before oxidation and polymerization are initiated. Such binding is confirmed by molecular dynamics (MD) simulations, supporting the assumption that the reactions which lead to poly(PADPA) are localized on the vesicle surface. The poly(PADPA) obtained resembles the emeraldine salt form of polyaniline (PANI-ES) in its polaron state with a high content of unpaired electrons, as judged from UV/vis/NIR, EPR, and FTIR absorption measurements. There are, however, also notable spectroscopic differences between PANI-ES and the enzymatically prepared poly(PADPA). Poly(PADPA) appears to be similar to a chemically synthesized poly(PADPA) as obtained in a previous work with ammonium peroxydisulfate (APS) as the oxidant in a mixture of 50 vol % ethanol and 50 vol % 0.2 M sulfuric acid (*J. Phys. Chem. B* **2008**, *112*, 6976−6987). ESI-MS measurements of early intermediates of the reaction with TvL and AOT vesicles indicate that the presence of the vesicles decreases the extent of formation of unwanted oxygen-containing species in comparison to the reaction in the absence of vesicles. This is the first information about the differences in the chemical composition of early reaction intermediates when the reaction carried out in the presence of vesicles under optimal conditions is compared with a template-free system.

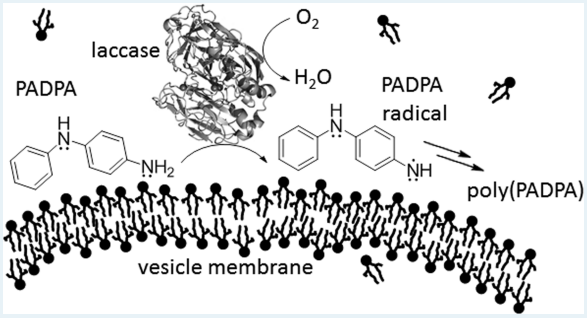

KEYWORDS: *aniline, enzyme, laccase, liposomes, p-aminodiphenylamine, polyaniline, polymer, vesicles*

INTRODUCTION

The investigation of the synthesis of polymers with peroxidases or laccases as a catalyst is an active area of research.[1−5] It is fascinating but also highly challenging, in particular if one aims at understanding the details of the molecular complexity of the reaction. In general, enzymatic polymerizations are promising because they can be carried out under mild conditions in aqueous media, thereby contributing to the development of environmentally friendly, atom-efficient polymerization processes.[6,7] On the other hand, the particular challenge in using oxidizing enzymes to initiate polymerization reactions often is to specifically control the outcome of the reaction so that desired polymers with a distinct chemical structure are obtained instead of ill-defined products.[3] Indeed, ill-defined reaction products may be obtained with peroxidases and laccases, depending on the type of monomers used and depending on the experimental conditions.[8,9] This unpleasant situation can be comprehended by considering the actual role which a peroxidase or laccase plays in the entire reaction, briefly outlined as follows. In contrast to a lipase-catalyzed polymer-

Received: June 4, 2014
Revised: August 19, 2014
Published: August 22, 2014

Scheme 1. Stoichiometric Equation for the Polymerization of PADPA into Poly(PADPA) with TvL as Catalyst and O_2 as Oxidant[a]

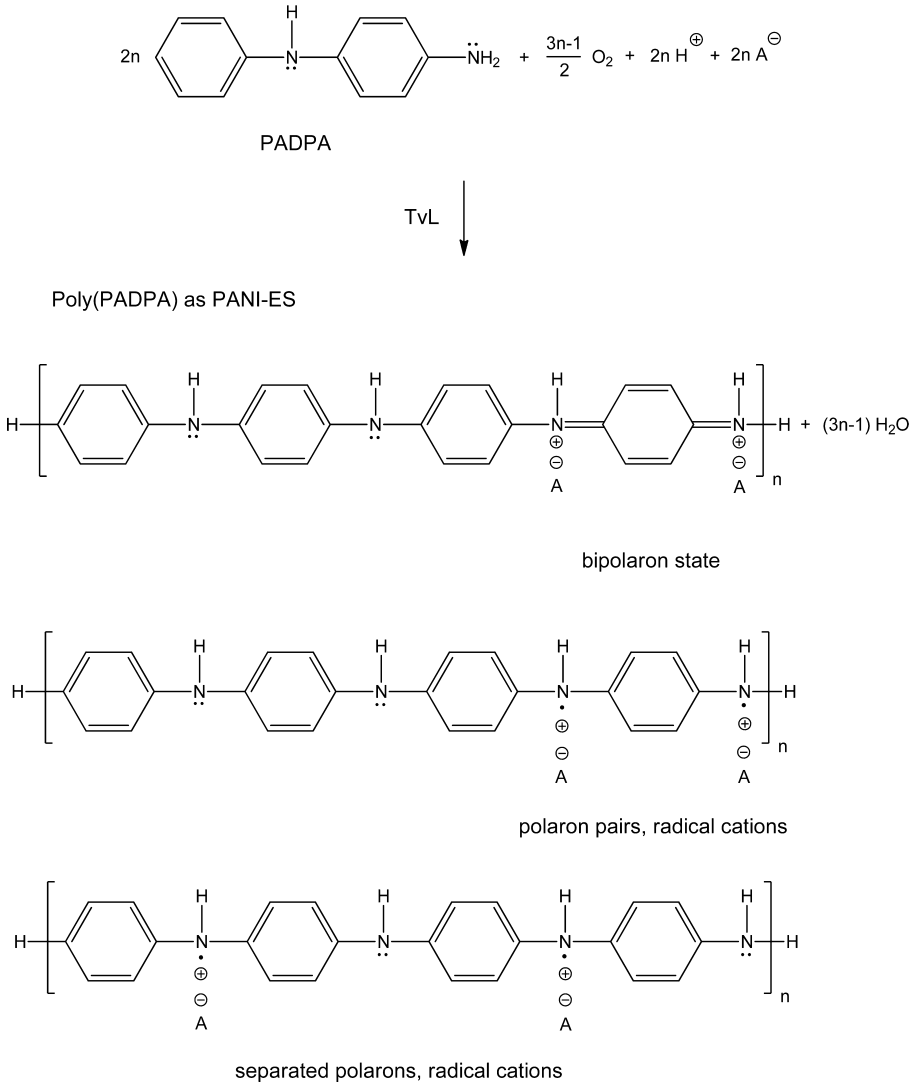

[a]Poly(PADPA) is represented as polyaniline in its emeraldine salt form (PANI-ES), shown with tetrameric aniline repeating units in their bipolaron or polaron states.[28,42] Polarons have unpaired electrons and are "EPR active".[42] Depending on the experimental conditions, n may vary from $n = 1$ to $n \gg 1$, and more importantly, other couplings of PADPA may also exist, leading to the formation of oligo- and poly(PADPA) products with $n = 3/2$, 5/2, etc. Furthermore, the formation of phenazine units is also possible, as well as other structural deviations from the ideal linear *para*-NC-coupled form shown.[28,43,44] A^- represents the counter ion, which in the system used probably mainly is the AOT anion.

ization reaction, for example, in which the active site of the lipase is directly involved in the coupling reactions leading to polymeric products, peroxidases and laccases solely oxidize monomers (or oligomers), presumably without direct participation of the enzyme's active site in the bond formation steps that lead to the polymers. Therefore, if various possibilities for the nonenzymatic coupling of oxidized monomers (or oligomers) exist, and if side reactions with the solvent may occur, it is expected that a complex mixture of different products is obtained. In this case, the addition of structure-directing templates—polymers, micelles, or vesicles—has proven to be a powerful tool for controlling the actual polymerization reaction in a desired way.[3,10−18] The presence of such templates leads to a localization of the reaction process in their vicinity, thereby increasing the extent of desired over unwanted coupling reactions. Moreover, the templates prevent the products from precipitating. One example is the recently investigated *Trametes versicolor* laccase (TvL)/O_2-catalyzed polymerization of aniline in the presence of vesicles formed from AOT (= sodium bis(2-ethylhexyl) sulfosuccinate) at pH = 3.5 in 0.1 M phosphoric acid−sodium dihydrogen phosphate solution and $T = 25$ °C.[19] Although the vesicles clearly served as templates for the reaction, three major drawbacks were recognized: (i) the reaction with aniline (Ar-NH_2) as the monomer is very slow, (ii) overoxidized products are obtained, and (iii) the laccase is unstable in diluted aqueous solution if kept for the long period of time required for the reaction (≈ 27 days at room temperature to reach high yields under the conditions used). One enzyme molecule was needed for the oxidation of about 750 aniline molecules[19] (corresponding to about 190 cycles, each involving four molecules of Ar-NH_2, one O_2 molecule, and the transferal of four electrons). The general difficulty in oxidizing aniline with laccases is mainly due to the low value of the standard potential for the oxidation of aniline

dx.doi.org/10.1021/cs500769d | *ACS Catal.* 2014, 4, 3421−3434

(E°_{ox} = −1.0 V for Ar−NH_2 → Ar−$NH_2^{\bullet+}$ + 1 e^-).[20] The reduction potential for TvL at pH = 2.5−7.0, $E^{\circ\prime}_{red}$, is only about 0.78 V ($Cu(II)_{T1}$ + 1 e^- → $Cu(+I)_{T1}$).[21,22]

In the work presented here, we show that replacing aniline with the aniline dimer *p*-aminodiphenylamine (PADPA, Ar−NH−*p*−Ar−NH_2) leads to an efficient formation of poly-(PADPA) at pH = 3.5 if the same type of AOT vesicles is used as templates as for the polymerization of aniline with the same laccase/oxidant system (i.e., TvL/O_2). The reaction with PADPA has several important advantages compared to the polymerization of aniline catalyzed by the same enzyme−vesicle system. First, PADPA is easier to oxidize than aniline: E°_{ox} for Ar−NH−*p*−Ar−NH_2→ Ar−NH−*p*−Ar−$NH_2^{\bullet+}$ + 1 e^- is about −0.4 V to −0.5 V,[23] as compared to E°_{ox} = −1.0 V for Ar-NH_2.[20] Second, the reaction with PADPA is much faster than with aniline. Third, laccase inactivation during the reaction with PADPA is much less severe as compared to the reaction with aniline. Overall, the amount of laccase required for the polymerization of PADPA is significantly lower than for the polymerization of aniline. In a previous study, Shumakovich et al.[24] already demonstrated that a laccase from *Trametes hirsuta* can be used efficiently for the polymerization of PADPA with micellar templates formed from sodium dodecylbenzenesulfonate at pH = 3.8.

The polymerization of PADPA with TvL/O_2 and AOT vesicles was optimized for obtaining a poly(PADPA) reaction product which resembles polyaniline in its conductive emeraldine salt form (PANI-ES, Scheme 1), with the characteristic UV/vis/NIR absorption spectrum of the polaron state. PANI-ES is one of the most intensively investigated conductive polymer due to its many applications in various fields[25−27] (e.g., for rechargeable batteries, for sensor devices, for anticorrosion coatings, etc). Poly(PADPA) was characterized by UV/vis/NIR-, EPR- and FTIR-spectroscopy and compared with (i) polyaniline obtained with the same laccase and the same vesicle templates but using aniline as monomer instead of PADPA; (ii) poly(PADPA) obtained by Shumakovich et al.[24] with *Trametes hirsuta* laccase and micellar templates; and (iii) poly(PADPA) obtained chemically with ammonium peroxydisulfate (APS) as oxidant.[28] Furthermore, molecular dynamics (MD) simulations were performed to shed some light on the interactions of PADPA with the AOT vesicle bilayer. A schematic representation of the entire vesicular reaction system used in this work is shown in Scheme 2.

Scheme 2. Schematic Representation of the Reaction System[a]

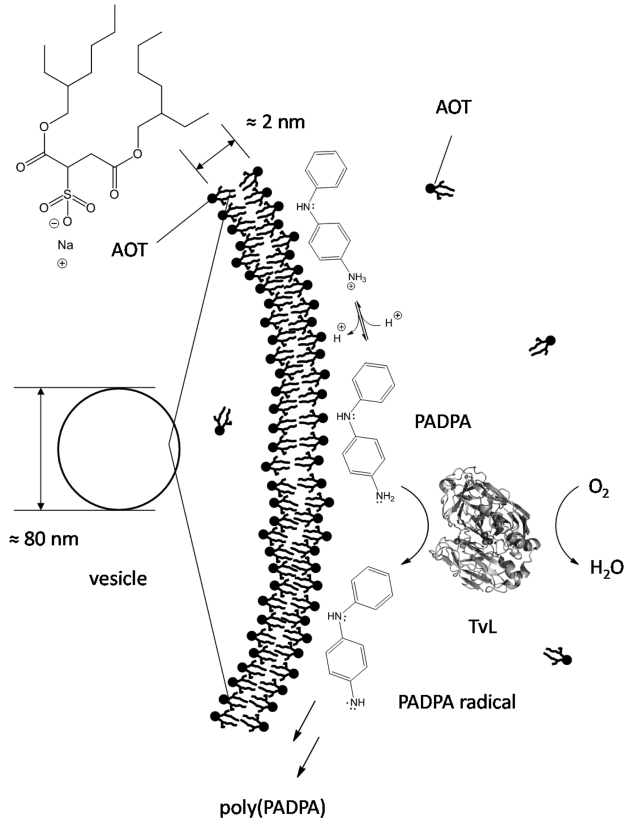

[a]The vesicles have a diameter of about 80 nm and are mainly unilamellar.[15,31] They are formed from AOT in aqueous solution in the presence of a mixture of H_3PO_4 and $H_2PO_4^-$ (0.1 M, pH = 3.5). Some of the AOT molecules are expected to exist in bulk solution and in the internal aqueous pool of the vesicles; the critical concentration for vesicle formation (cvc) is about 0.4 mM.[31] PADPA (at pH = 3.5 predominantly existing as Ar-NH-Ar-NH_3^+, pK_a = 4.70[37]) and the reaction intermediates and product, poly(PADPA), are localized preferentially in the area of the bilayer of the negatively charged vesicles. Glycosylated TvL is expected to distribute between the vesicle surface and the bulk solution, depending on the isoenzymes present in the crude laccase sample used; the reported pI values of the isoenzymes are between about 2.8 and 3.5[29,30,45] and between about 5.7 and 6.6.[45] TvL, PDB ID: 1GYC.[30] Assuming a one electron oxidation of PADPA by TvL/O_2, the stoichiometric equation for one catalytic cycle is 4 Ar-NH-Ar-NH_2 + O_2 + 4 H^+ → 4 Ar-NH-Ar-$NH_2^{\bullet+}$ + 2 H_2O.

MATERIALS AND METHODS

Chemicals. Laccase from *Trametes versicolor* (TvL, EC 1.10.3.2; product no. 51639, 13.6 U mg^{-1}, lot no. BCBF7247 V), sodium bis(2-ethylhexyl) sulfosuccinate (AOT ≥ 99%), diethyl ether (≥99.8%, GC), and PADPA (*p*-aminodiphenylamine, *N*-phenyl-1,4-phenylendiamine, 98%) were purchased from Sigma-Aldrich. Before use, PADPA was recrystallized two to three times from hexane until the product was colorless; stock solutions (1.5 mM) were freshly prepared on the day of use by dissolving the purified PADPA in pH = 3.5 solution in an ultrasound bath (see below), followed by adjustment of the pH with HCl to pH = 3.5. Methyl *t*-butyl ether (MTBE, ≥ 99.0%, GC) and sodium di-*n*-butylsulfosuccinate were from Fluka. All other chemical used were the same as in our previous work and used as received.[19]

Rough Estimation of the Molar Concentration of the Laccase. The content of active enzyme in the laccase stock solution prepared from the commercial laccase sample (12.9 mg/mL) was estimated as described previously.[19] First, the laccase activity was measured at pH = 3.0 with the substrate $ABTS^{2-}(NH_4^+)_2$, the diammonium salt of 2,2′-azino-bis(3-ethylbenzothiazoline-6-sulfonate), at various $ABTS^{2-}$ concentrations with a fixed amount of laccase. Then, the obtained extrapolated maximum reaction velocity (V_{max}, Michaelis−Menten kinetics) was related to the literature value for the turnover number for a purified isoenzyme TvL/$ABTS^{2-}$ at pH = 3.0 (k_{cat} = 220 s^{-1}, isoenzyme LacIIb with pI between 2.8 and 3.2).[29] In this way, the concentration of TvL in the laccase stock solution prepared (12.9 mg commercial TvL product dissolved in 1 mL of deionized water) was found to be ≈16 μM. This means that only about 8−9 wt % of the commercial laccase sample contained active enzyme, as calculated on the basis of a molar mass of TvL of 70 kDa.[30]

dx.doi.org/10.1021/cs500769d | ACS Catal. 2014, 4, 3421−3434

UV/vis/NIR and EPR Measurements of the Vesicle Suspensions. All UV/vis/NIR measurements were carried out with a JASCO V-670 spectrophotometer, and the EPR measurements of the vesicle suspensions with a Bruker EMX X-band spectrometer equipped with a TM cavity.[15]

Preparation of AOT Vesicles. AOT vesicles were prepared with the freeze−thawing polycarbonate membrane extrusion method by using a pH = 3.5 phosphate solution (0.1 M H_3PO_4 + NaH_2PO_4), as described previously.[19] The AOT concentration in the suspension was 20 mM and the average hydrodynamic vesicle diameter about 80 nm, as determined by dynamic light scattering measurements carried out immediately after vesicle preparation.[31] The vesicle suspension was stored protected from light at room temperature before use.

Interaction of PADPA with AOT Vesicles. The interaction of PADPA with AOT vesicles was analyzed by measuring the turbidity of a vesicle suspension (1.5 mM AOT, pH = 3.5) containing various amounts of PADPA. The samples were prepared by mixing defined volumes of a 20 mM AOT vesicle suspension (pH = 3.5), a 1.5 mM PADPA solution (pH = 3.5), and a pH = 3.5 solution (0.1 M H_3PO_4 + NaH_2PO_4) to obtain the desired concentrations of AOT and PADPA. After incubation for 1 h at room temperature, the turbidity of the samples was measured at λ = 600 nm by using a quartz cell with a path length of 1 cm.

Enzymatic Polymerization of PADPA with TvL in the Presence of AOT Vesicles. Polymerization reactions of PADPA with laccase/O_2 were carried out at pH = 3.5 at room temperature in 2 mL closed Eppendorf tubes with a reaction volume of 500 μL. The reaction vessel volume was 4 times the reaction volume. The reaction was started by mixing a pH = 3.5 solution (0.1 M H_3PO_4 + NaH_2PO_4), a vesicle suspension, a substrate stock solution, and an enzyme stock solution as follows (optimal conditions): 128.2 μL of pH = 3.5 solution (0.1 M H_3PO_4 + NaH_2PO_4), 37.5 μL of AOT vesicle suspension (20 mM, pH = 3.5 solution), 333.3 μL of PADPA stock solution (1.5 mM, pH = 3.5 solution); after mixing, the reaction was started by adding 1.0 μL of TvL stock solution (12.9 mg/mL ≈ 16 μM, deionized water). The initial concentrations in the reaction system were the following: 1.5 mM AOT, 1.0 mM PADPA, and ≈32 nM TvL. The required O_2 molecules for the reaction to occur were those available from the aqueous solution (0.5 mL) and from the air reservoir in the Eppendorf tube (1.5 mL). The typical reaction time was 24 h.

Polymerization reactions without vesicles were carried out in the same way, but instead of the vesicle suspension the same volume of the pH = 3.5 solution was added. For control measurements with sodium *n*-dibutylsulfosuccinate, a 20 mM stock solution of sodium *n*-dibutylsulfosuccinate was prepared and used instead of the 20 mM AOT vesicle suspension.

Laccase Activity Measurements during the Polymerization of PADPA. The activity of TvL in the reaction mixture was measured with 0.25 mM $ABTS^{2-}$ as substrate at pH = 3.5 (0.1 M H_3PO_4 + NaH_2PO_4) and T = 25 °C. Volumes of 15 μL were withdrawn from time to time from a 10 mL reaction mixture and then added into a 1 cm, 1.5 mL polystyrene cuvette to which 935 μL pH = 3.5 solution and 50 μL of an $ABTS^{2-}$ stock solution (5 mM prepared in pH = 3.5 solution) were first added. After gentle mixing, the solution was incubated for 7 min and then the increase in absorbance at λ = 414 nm, ΔA_{414}, originating from the formed $ABTS^{\bullet-}$ radical anion, was recorded for the following 3 min. A reproducible analysis during the first 7 min was not possible because often a lag phase with a nonlinear increase of A_{414} with time was observed. $\Delta A_{414}/\Delta t$ was taken as measure of the activity of TvL and the value determined for the reaction solution which was withdrawn 2 min after the start of the polymerization reaction was set to 100%.

ESI-MS Measurements. During PADPA polymerization, unreacted PAPDA and reaction products were extracted into a MTBE solution to which aqueous NH_3 was first added; the MTBE solution was then analyzed by ESI-MS. Details of the sample preparation and the MS analysis are given in the following. At predetermined times during the polymerization reaction (initial volume: 10 mL), 500 μL of the reaction mixture were withdrawn and added to 500 μL MTBE to which 50 μL of a 25 wt % aqueous NH_3 solution were first added. After vigorous shaking and waiting for phase separation, the colored lighter organic phase was separated and analyzed by ESI-MS, using an ESI-Q-TOF system (maXis, Bruker Daltonics, Germany) coupled with an Agilent 1200 system (Agilent Ltd., Germany). The MS instrument was operated in wide pass quadrupole mode with the TOF data being collected between m/z 50−1300 with a low-collision energy of 10 eV. The optimized source conditions were drying gas 8.0 L/h (nitrogen 99.99% purity) at a temperature of 200 °C, nebulizer pressure of 1.6 bar, capillary and end plate voltages of 500 and 4500 V, respectively, TOF flight tube voltage of 9867 V, reflection voltage of 1999 V, pusher voltage of 1638 V, and detector voltage of 3450 V. The resolving power of the instrument was around 35 000 with 2.5 Hz spectra rate. The ESI-TOF mass spectrometer was calibrated routinely for flow injection analysis (FIA) in the positive and negative electrospray ionization mode using Agilent-ESI-TOF tuning mix on the enhanced quadratic algorithmic mode. Further data processing was calculated using the Data Analysis 4.0 software (Bruker Daltonics, Germany).

Reference measurements were carried out with solutions that contained PADPA, AOT vesicles, or laccase samples only, or AOT vesicles together with laccase (instead of the reaction mixture).

Determination of the Consumption of PADPA during the Polymerization Reaction. The decrease in the amount of PADPA present in the reaction mixture as a function of reaction time was determined by ESI-MS, as described above. The EIC (extracted ion chromatograms) of signals between 183.09 and 186.11 ± 0.05 m/z were integrated between 1.0 and 1.3 min elution time. The value obtained for 2 min reaction time was set as 100%.

The EICs of reaction mixtures analyzed at different reaction times are shown in Figures S1 and S2, Supporting Information (SI). Scheme S1 (SI) shows possible chemical structures and calculated m/z values of the relevant detectable forms of PADPA that were taken into account for this determination, Ar−NH−Ar−NH_3^+, Ar−NH−Ar−$NH_2^{\bullet+}$, Ar−N$^{\bullet}$−Ar-$NH_2^{\bullet+}$, and Ar−N═Ar═NH_2^+.

Isolation of Poly(PADPA) and Analysis of Isolated Poly(PADPA). Poly(PADPA) was isolated by extraction with diethyl ether and MTBE from the reaction solution. All organic phases were combined, and the solvent was removed in vacuo. The remaining solid was treated with 1 M HCl solution for 30 min, afterward it was washed extensively with water and dried at high vacuum overnight. FTIR measurements of the isolated products were carried out with a Bruker Alpha instrument (KBr

dx.doi.org/10.1021/cs500769d | ACS Catal. 2014, 4, 3421−3434

pellet), and the EPR measurements were made with a ELEXSYS E580 instrument from Bruker, operated at X-band frequency, as described previously.[19,32] Conductivity and X-ray diffraction (XRD) measurements were performed in the same way as described previously.[19]

MD Simulations of AOT Bilayers. A patch of an AOT bilayer membrane composed of 16 × 16 × 2 AOT molecules was considered for simulation at T = 298 K, τ_t = 0.1 ps, and Berendsen thermostat[33] under periodic boundary conditions. The AOT bilayer was set up by including all eight possible stereoisomers of AOT; the use of a mixture of AOT stereoisomers for the simulation, instead of one type of AOT with particular configurations, reflects the real experimental situation and may be an important consideration, see the previous work of Horta et al.[34] For the individual AOT molecules, a polar headgroup area of 0.67 nm^2 was assumed, according to experimental data obtained by Grillo et al.[35] To compensate for surface tension, lateral pressure coupling in a range of $p_{lateral}$ = −18 to −45 bar was considered, but no equilibrium close to the headgroup area was reached. Therefore, a cubic box with isotropic pressure coupling, τ_p = 0.5 ps, p = 1 bar,[33] was established. NaH_2PO_4 and H_3PO_4 (0.1 M total concentration) were included according to pH. Some solvent molecules (water, SPC model)[36] were introduced or deleted after equilibration of 1 ns until little deviation from the experimental headgroup area was established. PADPA was introduced by λ perturbation during 1 ns after the pure membrane-buffer system was equilibrated for at least 20 ns. The equilibrium simulation was analyzed for 10 ns. Further details of the model, the protocol and details about the simulation of the AOT bilayer without any PADPA added are disclosed in the SI (Figure S3−S5, Tables S1−S4). The concentration of PADPA was chosen as 5 times higher than in the experiments, to gain better local statistics. The local concentration of AOT was 252 times higher than the experimental 1.5 mM due to the limited solvent volume.

RESULTS

Interaction of PADPA with AOT Vesicles. Mixing an AOT vesicle suspension at T = 25 °C with an aqueous solution of PADPA at pH = 3.5 led to an increase in turbidity of the vesicle suspension, the extent of turbidity increase being dependent on the concentrations of AOT and PADPA. This initial qualitative observation allowed us to investigate the interaction of PADPA with AOT vesicles turbidimetrically by measuring the optical density of a vesicle suspension, at the arbitrarily chosen wavelength of λ = 600 nm, as a function of the concentration of PADPA, see Figure 1. The AOT concentration was kept constant at 1.5 mM, the pH value was 3.5 (0.1 M H_3PO_4 + NaH_2PO_4), and the temperature was 25 °C. These were the conditions which we found to be optimal for the polymerization reaction (see below). Figure 1 shows that the turbidity of the vesicle suspension up to about 0.30−0.35 mM PADPA was low. Above 0.40 mM PADPA, there was a distinct increase in turbidity which could easily be seen by the naked eye. Without vesicles, the sample remained transparent up to at least 1.0 mM PADPA. Above about 2 mM, PADPA was no longer soluble at pH = 3.5.

PADPA interactions with AOT bilayers are supported by MD simulations (Figure 2A,B). The simulations were carried out with an AOT bilayer fragment, positioned horizontally in the center of the simulation box, and by taking into account pH = 3.5 conditions in the presence of H_3PO_4, $H_2PO_4^-$, and Na^+

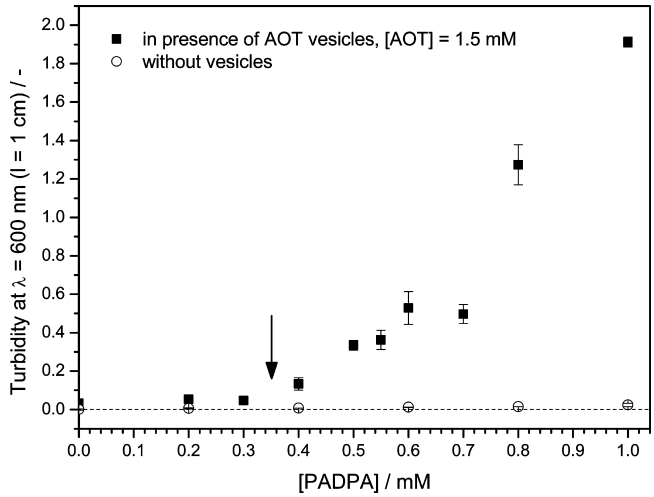

Figure 1. Effect of PADPA on the turbidity of the AOT vesicle suspension used (■); [AOT] = 1.5 mM, pH = 3.5 (0.1 M H_3PO_4 + NaH_2PO_4). (○): Control measurements without vesicles. The turbidity was measured at λ = 600 nm by recording the absorbance (path length: 1 cm). The data shown are mean values and standard deviations for three measurements at T = 25 °C. The arrow indicates the approximate start of the increase in turbidity which was at [PADPA] ≈ 0.35 mM.

species for mimicking the experimental situation as well as possible (see SI). At this pH value, the dominant species of PADPA is its protonated form Ar-NH-Ar-NH_3^+ (pK_a 4.7).[37] Therefore, all MD simulations were carried out by considering Ar-NH-Ar-NH_3^+.

As a first interesting finding, the simulations showed that the AOT bilayer—simulated without any added PADPA—has a bumpy surface and a partially disrupted structure (SI, Figure S5). The surface average maximal height minus the surface average minimal height of AOT leads to an estimate of 2.60 nm for the thickness of the AOT in the bilayer, comparable to the thickness obtained from SANS experiments (1.85 ± 0.8 nm).[15] An analysis of the simulated AOT bilayer in the presence of PADPA (Figure 2A,B) shows that along the normal z-axis, 100% of the AOT molecules are distributed within the central half of the box and that 87% of PADPA are found within the vicinity of AOT. Such PADPA binding to the AOT bilayer is reasonable because it reflects the experimental observations made (see above) and agrees with the known low water solubility of PADPA.[28] In contrast to PADPA, over two-thirds (69%) of H_3PO_4 and $H_2PO_4^-$ are found in the AOT-free solvent half of the simulation box, that is, they are part of the bulk aqueous solution, as expected. The MD simulations indicate that PADPA is partially inserted into the AOT bilayer and has some orientation, see the side view shown in Figure 2B. We calculated the angular distribution of PADPA and found that 30−45° (and 135−150°) tilt angles are preferred (Figure 2C). A tilt angle of 90° means that the PADPA alignment is perpendicular to the bilayer normal. This situation clearly does not dominate.

Overall, the MD simulations indicate that PADPA integrates into the membrane, rather than lying flat on the surface. Although there is uncertainty about the real molecular situation with respect to the PADPA-AOT bilayer interaction, the MD simulations provide some hints about how the situation might be. For example, Ar-NH-Ar-NH_3^+ was found to be involved in hydrogen binding as follows: on average per time frame, one

dx.doi.org/10.1021/cs500769d | ACS Catal. 2014, 4, 3421−3434

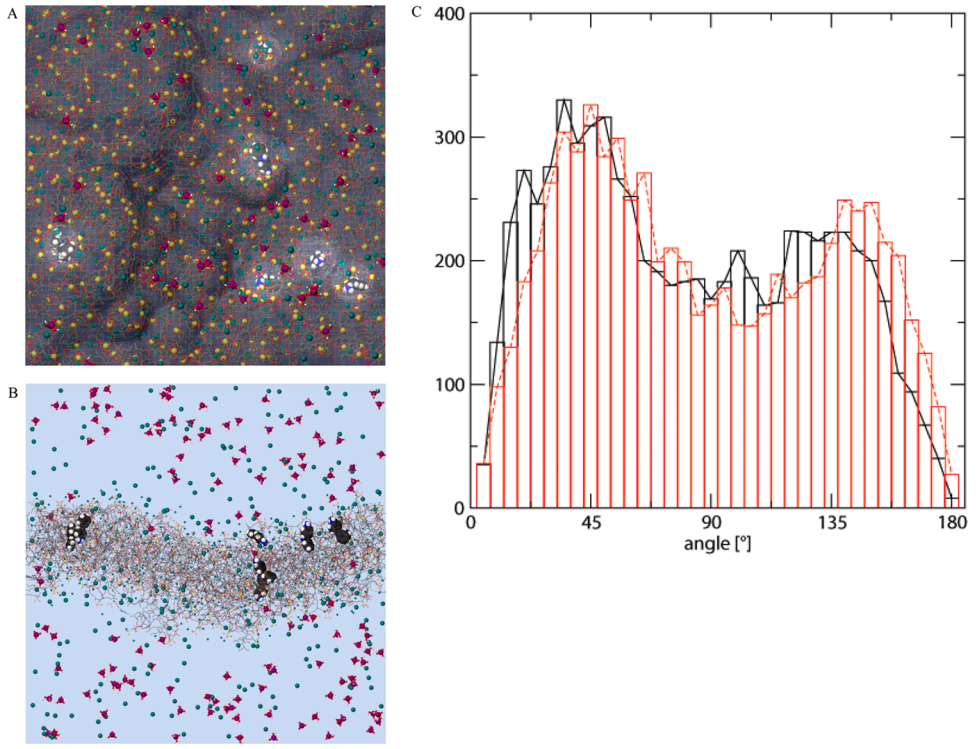

Figure 2. Molecular dynamics simulation of 5 mM PADPA dissolved in the AOT suspension at pH = 3.5 (0.1 M H_3PO4 + NaH_2PO_4). (A) Top view, 87% of the PADPA molecules are found to be associated with AOT within 10 ns of simulation. Hydrogen bonding of the amine group to the solvent is preferred—it is often exposed to the surface. (B) Side-view of PADPA "dissolved" in the AOT suspension. PADPA is shown as space filling model. AOT is displayed as thin-wire drawing, and sodium counterions in vicinity of AOT are sketched as smaller spheres. (C) Distribution of angles of PADPA orientation dissolved in the AOT suspension within 10 ns of simulation. The angle between the longitudinal axis of PADPA and the *z*-axis of the box (red) or the normal axis perpendicular to the local elevation of the membrane (black) has been calculated.

Ar-NH-Ar-NH_3^+ hydrogen bonded to 3.2 water molecules, to 1.0 AOT and to 0.1 of the phosphates. The presence of hydrogen bonds is further supported by additional analysis of the radial distribution functions with respect to the acidic oxygen of AOT and the water oxygen. In PADPA, of the two amines, only the exposed and protonated amine end group is unambiguously bonded to water, whereas both amines are hydrogen bonded to the oxygen atoms of AOT.

Formation of Poly(PADPA) with *Trametes versicolor* Laccase (TvL)/O_2 and AOT Vesicles as Templates, as Monitored by UV/vis/NIR and EPR Measurements. The optimal conditions for the polymerization of PADPA to poly(PADPA) with TvL/O_2 as catalyst and oxidant and AOT vesicles as templates were found to be 1.5 mM AOT, 1.0 mM PADPA, [TvL] ≈ 32 nM, pH = 3.5 (0.1 M H_3PO_4 + NaH_2PO_4), T = 25 °C, t = 24 h. They were judged to be optimal on the basis of the following criteria: (i) high absorption of the reaction products in the NIR-region of the absorption spectrum (around 1000 nm) and concomitant low absorption at about 500 nm, which can be considered as an indication for the formation of products that resemble the conductive dark-green emeraldine salt form of polyaniline (PANI-ES) in its polaron state,[15,38] see Scheme 1; (ii) high yield (i.e., high PADPA conversion as determined by ESI-MS, see Materials and Methods, and high absorbance at $\lambda \approx 1000$ nm); and (iii) use of small amounts of TvL. With respect to this last criterion, the effect of the TvL concentration on the absorption spectrum of the reaction products obtained after 24 h reaction time was investigated. The reaction mixture initially contained 1.5 mM AOT, 1.0 mM PADPA and various amounts of TvL at pH = 3.5, see SI, Figure S6. On the basis of these measurements, the optimal enzyme concentration was found to be 32 nM (2.0 μL TvL stock solution added per mL), see Figure 3 and SI, Figure S6H. With this TvL concentration and 1.0 mM PADPA, 1.5 mM AOT (pH = 3.5), the changes in the absorption spectrum between 220 and 1200 nm were measured during the polymerization reaction as a function of time. The spectra recorded after 2 min, 30 min, 1, 2, 3, and 4 h are shown in Figure 4A,B, and the spectrum recorded after 24 h, with its maxima at 1014, 421, and 306 nm, is shown in Figure 3. When the reaction was conducted without vesicles or in the presence of 1.5 mM sodium di-*n*-butylsulfosuccinate, which at this concentration neither forms vesicles nor micelles,[15] the spectra recorded during the polymerization were very different, see SI, Figure S7 and Figure S8. This clearly demonstrates the important role of the vesicular aggregates as templates.

In addition to recording UV/vis/NIR absorption spectra, EPR spectra were also measured during the polymerization in the presence of AOT vesicles, see Figure 5. The appearance of an EPR signal during the reaction indicates that the products contained unpaired electrons, as expected for a poly(PADPA) product which resembles PANI-ES in its polaron state, see Scheme 1. When the reaction was conducted without vesicles but under otherwise identical conditions—or in the presence of 1.5 mM sodium di-*n*-butylsulfosuccinate instead of AOT vesicles—the obtained reaction products had a very low content of unpaired electrons, see SI, Figure S9. This again confirms the importance of the presence of vesicles for obtaining products with the desired characteristics.[3]

dx.doi.org/10.1021/cs500769d | *ACS Catal.* 2014, 4, 3421−3434

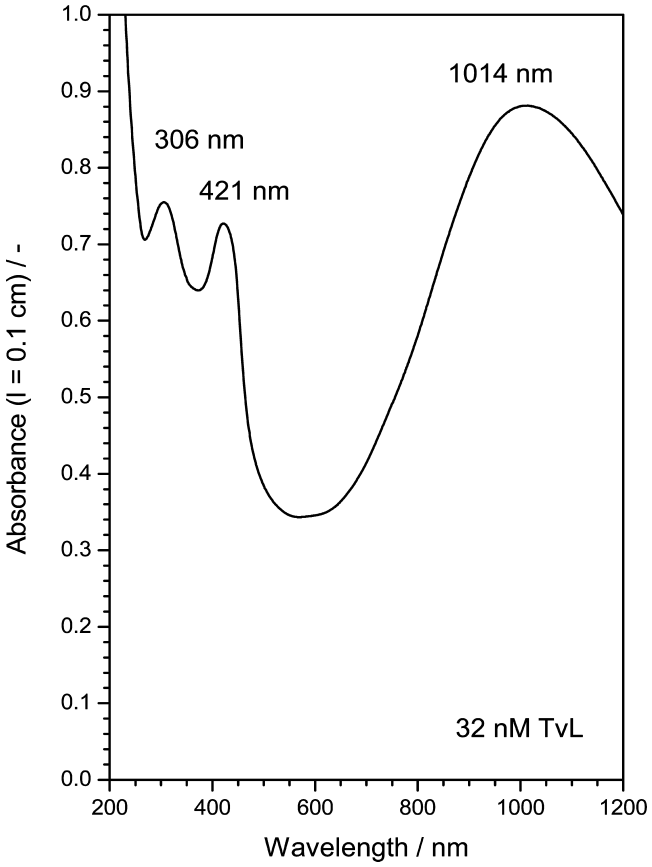

Figure 3. Polymerization of PADPA in the presence of AOT vesicles as templates and TvL/O_2 as catalyst and oxidant with [TvL] = 32 nM. UV/vis/NIR absorption spectrum of the reaction products obtained after a reaction time of 24 h at room temperature ($T \approx 25$ °C). [AOT] = 1.5 mM, $[PADPA]_0$ = 1.0 mM, pH = 3.5 (0.1 M H_3PO_4 + NaH_2PO_4). The amount of laccase used was 2.0 μL laccase stock solution (12.9 mg per mL deionized water) added to 1 mL of a buffered suspension of AOT vesicles (pH = 3.5) containing the substrate PADPA. Total volume of the reaction mixture: 1.0 mL. Reaction vessel: 5 mL polypropylene Eppendorf tubes with closed stopper.

PADPA Conversion and Changes in TvL Activity during PADPA Polymerization. Addition of methyl-*t*-butyl ether (MTBE) to samples withdrawn from the aqueous reaction mixture during the polymerization led to an extraction of PADPA and some reaction products into the organic phase. During this extraction, the intensity of the green color of the aqueous reaction mixture became very weak, whereas at the same time, the organic phase turned purple. Analysis of the MTBE soluble compounds by ESI-MS indicated that about 35% PADPA remained after a reaction time of 1 h, although after 4 h, almost all of the initially present PADPA was consumed (about 1% left), see Figure 6. Analysis of the reaction carried out in the absence of the vesicles showed a somewhat faster decrease in the amount of PADPA with time (13% left after 1 h, less than 1% after 4 h).

The activity of TvL was measured with $ABTS^{2-}$ as the substrate during the polymerization reaction by withdrawing samples from the reaction mixture from time to time, see Materials and Methods. The results are shown in Figure 7. Similar measurements were carried out for a reaction in the absence of AOT but otherwise identical conditions, or in the presence of sodium di-*n*-butylsulfosuccinate instead of AOT,

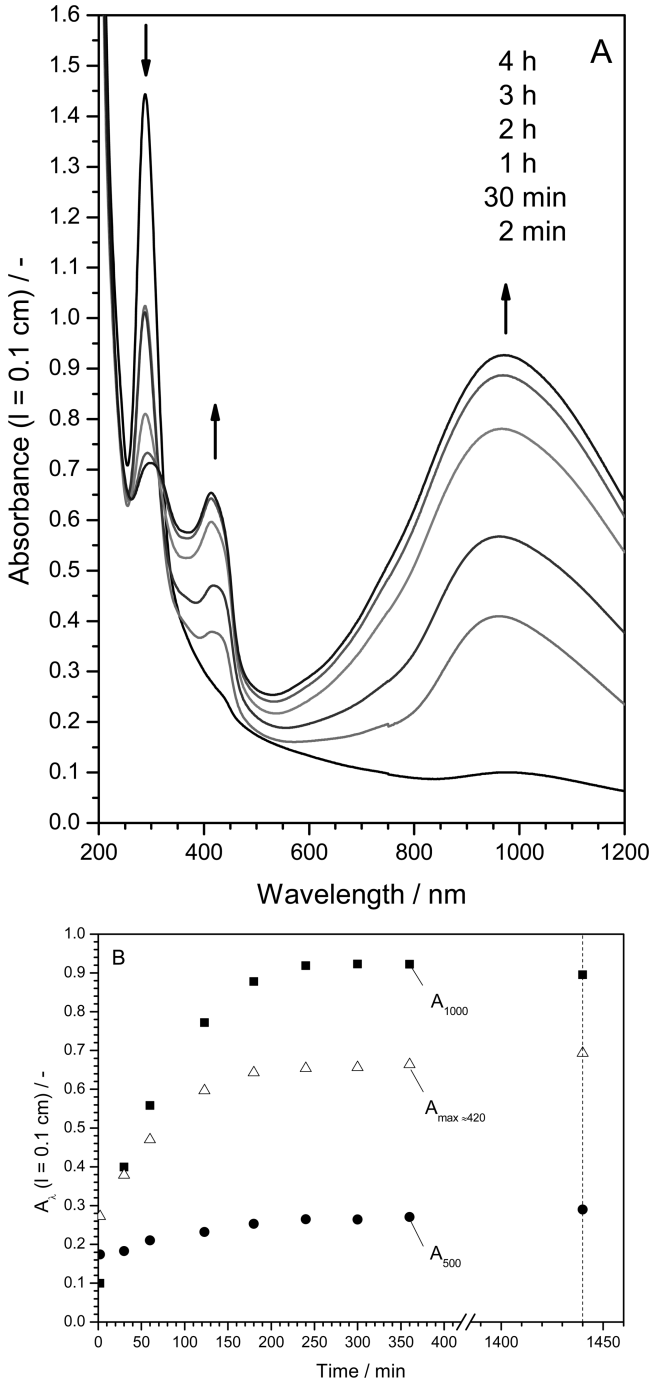

Figure 4. Polymerization of PADPA in the presence of AOT vesicles as templates and TvL/O_2 as catalyst and oxidant. Time-dependent changes of the UV/vis/NIR absorption spectrum of the reaction mixture for [AOT] = 1.5 mM, $[PADPA]_0$ = 1.0 mM, pH = 3.5 (0.1 M H_3PO_4 + NaH_2PO_4), $T \approx 25$ °C. [TvL] = 32 nM, see legend of Figure 3. Total volume of the reaction mixture: 15.0 mL. Reaction vessel: 50 mL Schott Duran glass bottle with screw cap. Samples were withdrawn, and the absorption spectrum was measured with a 0.1 cm quartz cuvette. (A) Spectra recorded after a reaction time of 2 min, 30 min, 1, 2, 3, and 4 h. The changes in the spectra correlate with the sequence of the reaction time as indicated. (B) Changes of the absorbance at λ = 1000 nm (■, A_{1000}), at λ = 500 nm (●, A_{500}), and at $\lambda_{max} \approx 420$ nm (Δ, $A_{max\approx_{420}}$). The dotted line indicates the chosen reaction time, t = 24 h, considered to be optimal for the continuation of the investigation.

dx.doi.org/10.1021/cs500769d | *ACS Catal.* 2014, 4, 3421−3434

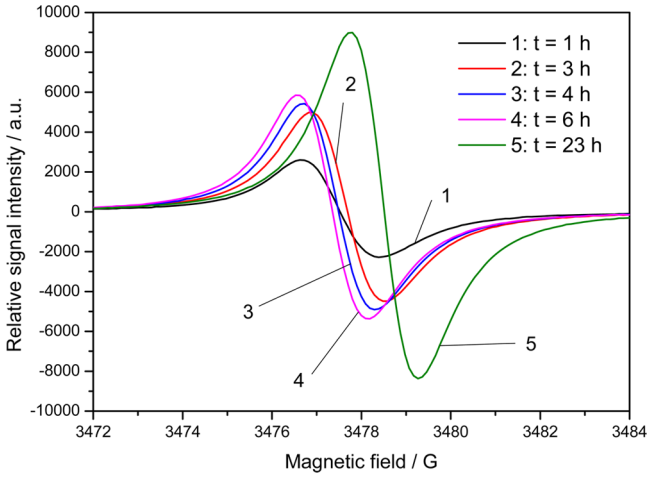

Figure 5. Polymerization of PADPA in the presence of AOT vesicles as templates and TvL/O_2 as catalyst and oxidant. Time-dependent changes of the EPR spectrum of the reaction mixture for [AOT] = 1.5 mM, $[PADPA]_0$ = 1.0 mM, pH = 3.5 (0.1 M H_3PO_4 + NaH_2PO_4), $T \approx 25$ °C. [TvL] = 32 nM, see legend of Figure 3. Total volume of the reaction mixture: 1.0 mL. Reaction vessel: 5 mL of polypropylene Eppendorf tubes with closed stopper. Samples were measured with a flat quartz cell. The spectra were recorded after a reaction time of 1 h (1), 3 h (2), 4 h (3), 6 h (4), and 23 h (5).

see SI, Figure S10. In all cases, the enzyme activity decreased with time. However, about 40% of the initial laccase activity was still present after 6 h, when practically all of the PADPA had been consumed, see above. Therefore, there were always enough active enzyme molecules present for oxidizing the remaining PADPA.

Preliminary Analysis of Early Reaction Intermediates by ESI-MS. As mentioned above, compounds soluble in MTBE were analyzed by ESI-MS during the polymerization reaction to determine the PADPA conversion, see Figure 6. Although a detailed analysis of the extractable reaction products would be beyond the topic of this paper, and is part of a detailed follow-up study, the ESI-MS spectra obtained after a reaction time of 31 min indicate that there are significant differences between the reaction products formed in the presence of vesicles as compared to the reaction carried out without vesicles. Without vesicles, molecules that contain oxygen are detected, whereas during the reaction with vesicles, such oxygen-containing compounds could not be identified. Figure 8 shows a small section of the ESI-MS spectrum where the differences can be clearly seen (region of m/z = 183.6−186.5). Figure 8A is the ESI-MS spectrum of the extractable compounds obtained from the reaction in the presence of AOT vesicles, whereas Figure 8B is the ESI-MS spectrum of the MTBE-soluble compounds obtained from the reaction carried out without any vesicles. In the latter, the peaks at 184.0756 m/z and 185.0795 m/z indicate presence of Ar-NH-Ar−OH^+ (Figure 8B). These peaks are absent in the spectra of the MTBE extracts obtained from the reaction mixtures with AOT vesicles (Figure 8A).

Characterization of Poly(PADPA). After isolation of poly(PADPA) obtained under the optimal reaction conditions with the AOT vesicles as templates (1.5 mM AOT, 1.0 mM PADPA, 2 μL/mL TvL, pH = 3.5 (0.1 M H_3PO_4 + NaH_2PO_4), $T \approx 25$ °C, t = 24 h), the FTIR spectrum of the isolated and purified product was measured, see Figure 9 for the recorded spectrum and Table 1 for the assignments of the bands based on literature. The spectrum had the characteristic bands one

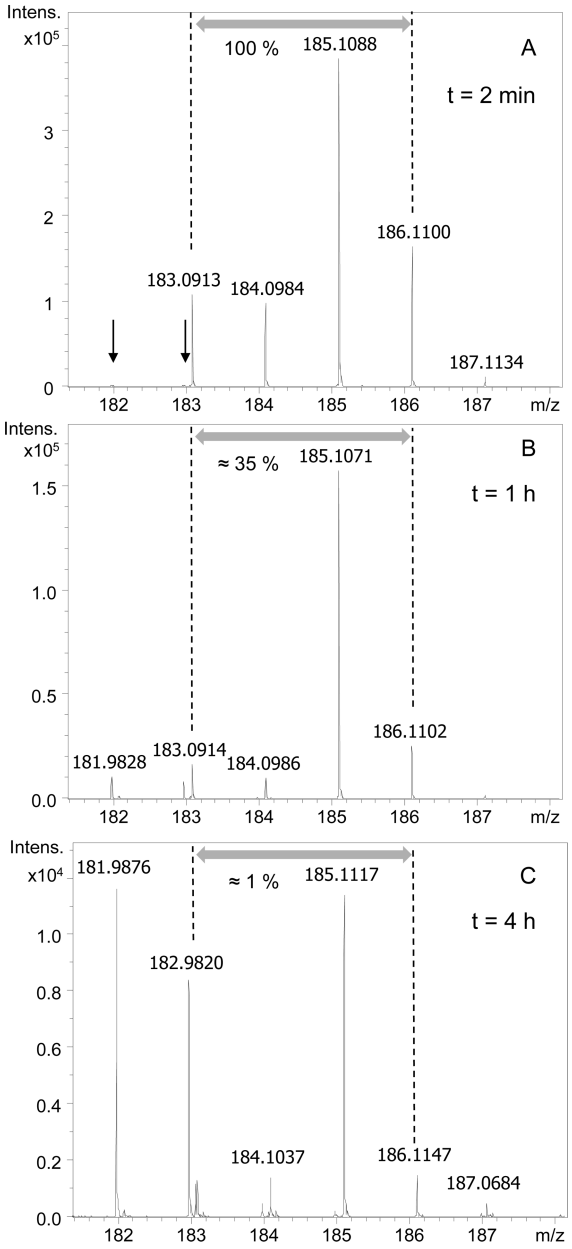

Figure 6. Polymerization of PADPA in the presence of AOT vesicles as templates and TvL/O_2 as catalyst and oxidant. ESI-MS analysis of the MTBE soluble compounds showing the signals detected between 181.4 and 188.2 m/z, arising partially from the cationic forms of PADPA ($C_{12}H_{11}N_2^+$: m/z = 183.0922, 184.0956; $C_{12}H_{12}N_2^+$: m/z = 184.1000, 185.1034; $C_{12}H_{13}N_2^+$: m/z = 185.1079, 186.1112), see SI, Scheme S1. [AOT] = 1.5 mM, $[PADPA]_0$ = 1.0 mM, pH = 3.5 (0.1 M H_3PO_4 + NaH_2PO_4), $T \approx 25$ °C. [TvL] = 32 nM, see legend of Figure 3. Total volume of the reaction mixture: 10 mL. Reaction vessel: 50 mL Schott Duran glass bottle with screw cap. The reaction times were 2 min (A), 1 h (B), and 4 h (C). The ECI of the signals between (183.09−186.11) ± 0.05 m/z, indicated with dashed lines, were integrated between 1.0 and 1.3 min elution time, yielding the indicated relative amounts of PADPA after 1 h (≈ 35%) and after 4 h (≈ 1%); the value measured after 2 min was taken as 100%. The two arrows in A point to the low intensities of the two peaks at 181.98 and 182.98 m/z.

expects for the functional groups present in the emeraldine salt form of PANI in its polaron state, for example, the C═C stretching vibrations at 1572 cm^{-1} (quinoid diimine) and

dx.doi.org/10.1021/cs500769d | ACS Catal. 2014, 4, 3421−3434

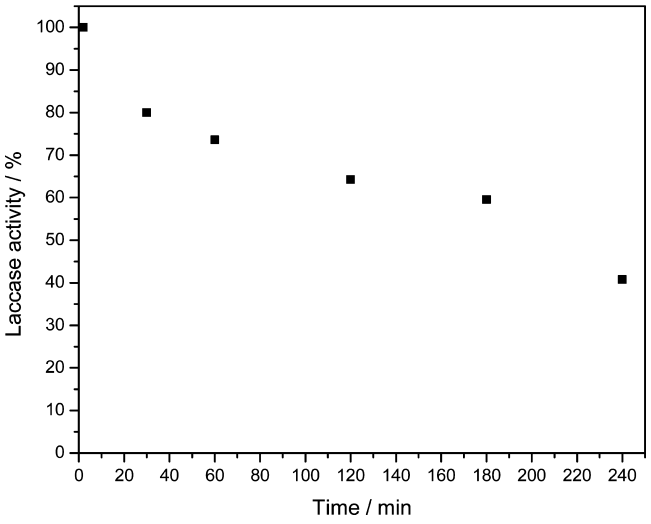

Figure 7. Polymerization of PADPA in the presence of AOT vesicles as templates and TvL/O_2 as catalyst and oxidant. Changes of the laccase activity during the reaction. [AOT] = 1.5 mM, $[PADPA]_0$ = 1.0 mM, pH = 3.5 (0.1 M H_3PO_4 + NaH_2PO_4), $T \approx 25$ °C. [TvL] = 32 nM, see legend of Figure 3. Total volume of the reaction mixture: 10 mL. Reaction vessel: 50 mL Schott Duran glass bottle with screw cap, slightly stirred with a magnetic stirrer bar. The activity of laccase was measured with $ABTS^{2-}$ as substrate, see Materials and Methods.

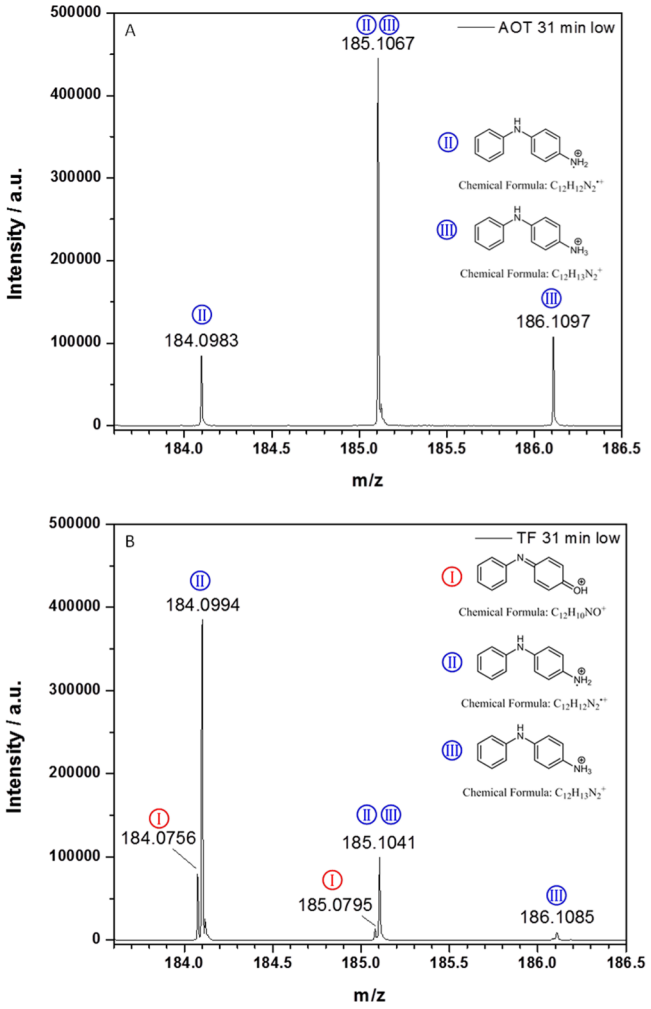

Figure 8. ESI-MS analysis of the MTBE soluble compounds extracted after a reaction time of 31 min. Shown is the range between 183.6 *m*/*z* and 186.5 *m*/*z*. (A) Reaction with AOT vesicles, [AOT] = 1.5 mM, $[PADPA]_0$ = 1.0 mM, pH = 3.5 (0.1 M H_3PO_4 + NaH_2PO_4), $T \approx 25$ °C. [TvL] = 32 nM, see legend of Figure 3. (B) Reaction without vesicles, but otherwise identical conditions as for A. The tentative assignment of the signals is given with the inserted chemical structures.

around 1500 cm^{-1} (1506 and 1495 cm^{-1}, benzenoid diamine), the bands at 1156 and at 1243 cm^{-1}, which are assigned to C−H and C−N stretching vibrations in subunits expected to be present in the molecule. The bands at 1734 and 1034 cm^{-1} show that a substantial amount of AOT was still contained in the isolated product which is obtained following the purification steps described in Materials and Methods.

The isolated solid poly(PADPA) sample was analyzed by EPR spectroscopy in the same way as described previously.[32] It was found that there are significant differences between poly(PADPA) obtained with AOT vesicles and TvL/O_2, abbreviated as poly(PADPA)-TvL-AOT (this work), and polyaniline obtained with TvL/O_2 or HRPC/H_2O_2 (HRPC: horseradish peroxidase isoenzyme C) and AOT vesicles (PANI-TvL-AOT and PANI-HRPC-AOT).[32] The estimated spin concentration determined at room temperature for poly(PADPA)-TvL-AOT (1.98×10^{20} spin/g) was between the one found for PANI-TvL-AOT (1.47×10^{20} spin/g)[32] and the one for PANI-HRPC-AOT (3.36×10^{20} spin/g).[29] The peak-to-peak line width (Δ_{pp}), the ratio of the peak amplitudes expected for a Dyson line shape (a/b), and the *g*-value were 0.26 mT, 1.03, and 2.0056 for poly(PADPA)-TvL-AOT, as compared to 0.28 mT, 1.21, and 2.0046 for PANI-TvL-AOT,[32] or 0.41 mT, 1.209, and 2.0055 for PANI-HRPC-AOT,[32] respectively. Differences between poly(PADPA) and the previously obtained PANI samples become very obvious if the temperature dependency of their EPR spectra is compared, as shown in Figure 10A,B. In these panels, data for PANI-TvL-AOT are also plotted for direct comparison. For a comparison with PANI-HRPC-AOT, see Rakvin et al.[32] The order of magnitude for the J_1 and J_2 values obtained coincides with the expected values from quantum chemical calculations for aniline dimers and tetramers with corresponding conformations for singlet−triplet transitions in relative short sections of the polymer chain.[39] The parameters describing qualitatively possible bands of polaron interactions show significant differences in the band structure between poly(PADPA)-TvL-AOT and PANI-TvL-AOT. In the case of poly(PADPA)-TvL-AOT, the bands with lower *J* values, compared to the *J* values of PANI-TvL-AOT, contribute more to the total distribution of polaron interaction. It is assumed that polarons with higher *J* values appear due to an increased local disorder. Thus, EPR intensity measurements indicate that poly(PADPA)-TvL-AOT exhibits a lower percentage of "locally disordered dimers" in comparison to PANI-TvL-AOT and PANI-HRPC-AOT polymers. It is also noted that poly(PADPA)-TvL-AOT contains the largest amount of Curie contribution, C_0, that accounts for noncorrelated spins, in comparison to the other two PANI samples obtained enzymatically in the presence of AOT vesicles. For low-dimensional systems, such as conducting polymers, one expects a complex temperature dependency due to various types of relaxation mechanisms and their different contributions at different temperatures. The temperature dependency of the EPR line width for typical conductive polymers (PANI-ES)[32] indeed shows two prominent ranges of temperature dependency where the line width decreases in the low temperature interval with increasing temperature (5−20 K)

dx.doi.org/10.1021/cs500769d | ACS Catal. 2014, 4, 3421−3434

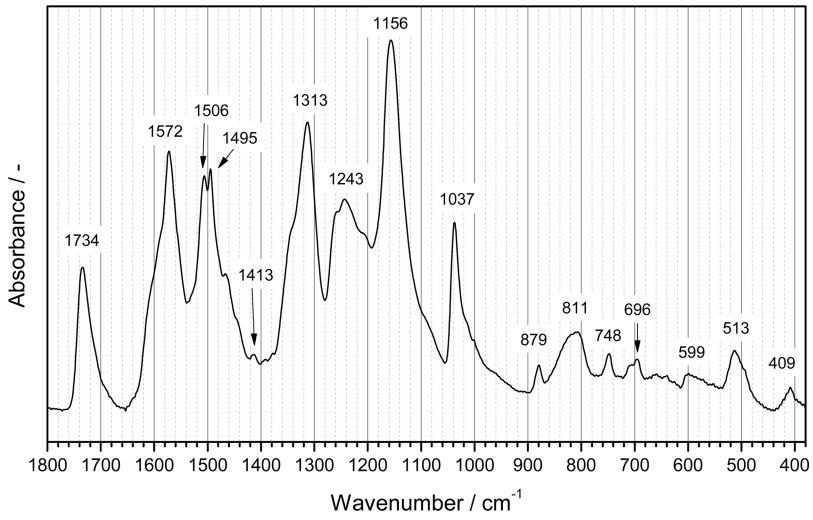

Figure 9. FTIR spectrum of the polymeric reaction products isolated after a reaction time t = 24 h. [AOT] = 1.5 mM, $[PADPA]_0$ = 1.0 mM, pH = 3.5 (0.1 M H_3PO_4 + NaH_2PO_4), $T \approx 25$ °C. [TvL] = 32 nM, see legend of Figure 3. Total volume of the reaction mixture: 300 mL. Reaction vessel: 1 L Schott Duran glass bottle with screw cap. The products were isolated from the reaction mixture by extraction into diethyl ether and MTBE, followed by work as described in Materials and Methods. The isolated products were grinded with KBr and pressed into a pill.

Table 1. Assignments of the IR Bands between 1800 and 400 cm^{-1} for the Poly(PADPA) Product Obtained with TvL/O_2 and AOT Vesicles as Templates[a]

wavenumber, cm^{-1}	assignment[b,c]
1734	from AOT, C═O (ν)
1037	from AOT, S═O (ν)
1572	C═C (ν) in N═Q═N
1506, 1495	C═C (ν) in N−B−N
1413	C═C (ν) in phenazines
1313	C−N (ν) in secondary aromatic amines or N−H (δ)
1243	$C-N^{\bullet+}$ (ν) in polaron lattice
1156	C−H (δ) in $Q{=}NH^{+}$-B or $B\text{-}NH^{\bullet+}$-B
879	C−H (γ) in 1,2,4-trisubstituted rings or in phenazines
811	C−H (γ) in 1,4-disubstituted rings
748	C−H (γ) in monosubstituted or 1,2-disubstituted rings
696	out-of-plane ring bending in monosubstituted rings
599	skeletal vibration in phenazines
513	out-of-plane ring deformation in 1,4-disubstituted rings or in monosubstituted rings
409	out-of-plane ring deformation

[a]Reaction conditions, see legend of Figure 9. [b]ν, stretching; δ, bending; γ, ring deformation; Q, quinoid ring; B, benzenoid ring. [c]Assignments based on refs 28, 42, 46, 15, and 16 (for AOT).

and a sharp increase with increasing temperature at higher temperatures. As was discussed earlier,[32] the narrowing behavior originates from the increase in population of triplet states with a singlet−triplet energy difference J comparable to the excitation energy of kT. The same mechanism leading to line width decrease could be applied to describe a monotonous line narrowing for all polymers obtained in the presence of AOT vesicles with increasing temperature for the entire temperature interval (5−300 K) monitored. We noted that for PANI-TvL-AOT and poly(PADPA)-TvL-AOT EPR line widths can be described with different activation processes, ΔE (detected as different possible slopes shown in Figure 10B), which are related to the energy for singlet to triplet transitions. Thus, the above analysis indicates that the inhomogeneously broadened EPR spectrum of these polymers at low temperatures contains distributions of spectral lines which originate from the distribution of triplet states. The lowest excited triplet state obtained at the low temperature limit is larger for poly(PADPA)-TvL-AOT (ΔE = 4.26 K) than for PANI-TvL-AOT (ΔE = 1.40 K). The plot in Figure 10B also clearly indicates the difference in variation of ΔE in this low temperature interval, and it could be connected to the different distribution of possible J values for the two polymers in this low temperature region. The role of the different distribution of J values—which is also suggested by the description of the susceptibility measured by EPR (Figure 10A) or line widths (Figure 10B)—could be related to an order of dimensionality of the polymer and/or to a local disorder. A recent example[40] for an oriented PANI based type of polymer in the form of thin films could be used as a more quantitative example to gather information on possible anisotropy and distribution of J values. The orientation-dependent susceptibility obtained from EPR of the polymer film was described by a localized state in which the spin 1/2 polarons behave as spin 1/2 dimers. The signature of anisotropy is assigned to anisotropy of the intradimer (J) and the interdimer (J') exchange values, along ($J_{\|}$ ~138 K, $J'_{\|} \sim \leq$

dx.doi.org/10.1021/cs500769d | ACS Catal. 2014, 4, 3421−3434

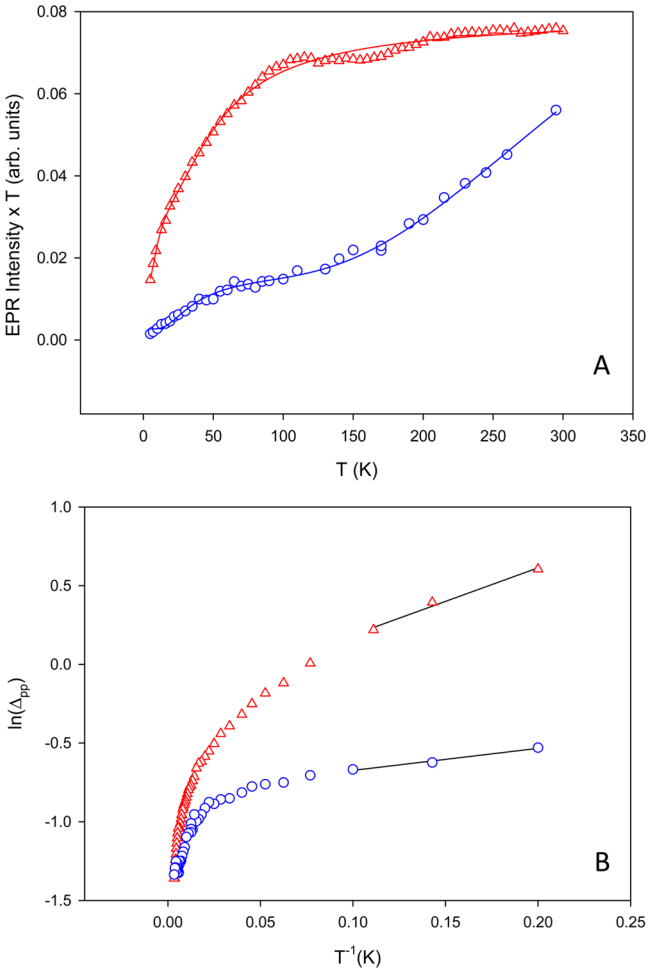

Figure 10. EPR analysis of poly(PADPA)-TvL-AOT in comparison with PANI-TvL-AOT. (A) EPR intensity multiplied with temperature plotted as a function of temperature for poly(PADPA)-TvL-AOT (open triangles) and for PANI-TvL-AOT (open circles, data from Rakvin et al.[32]), respectively. The continuous lines represent fits of the experimental data to eq 1[32] and the given fitting parameters

$$\chi T = C_0 + 4C_1/\left(3 + \exp\left(\frac{J_1}{k_B T}\right)\right) + 4C_2/\left(3 + \exp\left(\frac{J_2}{k_B T}\right)\right) + \ldots \quad (1)$$

whereby $C_i = N_i g^2 \mu_\beta S(S+1)/3k$ with $N_0 = (13.6 \pm 1.9) \times 10^{-3}$ spins/2-rings, $N_1 = (28.0 \pm 1.9) \times 10^{-3}$ spins/2-rings, $J_1 = 22 \pm 3$ K, $N_2 = (37.9 \pm 2.2) \times 10^{-3}$ spins/2-rings, $J_2 = 108 \pm 5$ K, for poly(PADPA)-TvL-AOT. For PANI-TvL-AOT, see Rakvin et al.[32] **B:** Natural logarithm of the EPR line width as a function of inverse temperature (T^{-1}), for poly(PADPA)-TvL-AOT (open triangles) and PANI-TvL-AOT (open circles, data from Rakvin et al.[32]), respectively. The activation process (ΔE) at low temperature, as calculated from the line widths (Δ_{pp} α $\exp(-\Delta E/kT)$), is 4.26 K for poly(PADPA)-TvL-AOT and 1.40 K for PANI-TvL-AOT.

66 K) and perpendicular ($J_\perp$ ~102 K, $J'_\perp \leq$ 48 K) to the polymer chain. This results in a gap defined as the energy difference between the bottom of the triplet band and the fundamental singlet state ($\Delta \approx J - 2J' \sim 7$ K). It is interesting to note that the magnitude of these J values and their anisotropy are variable in the close interval of J_1 and J_2 values in the present experiment for poly(PADPA)-TvL-AOT. Moreover, following the model described above, the lowest excited triplet state obtained at the low temperature limit of the EPR line width determinations could be correlated with the parameter Δ. In addition, it follows that for significantly larger values of J, the values mentioned above (such as J_2 = 752 K for PANI-TvL-AOT or J_2= 1133 K for PANI-HRPC-AOT polymers), could be more safely related to local disorder in the polymer structure as was discussed previously.[32]

The conductivity of poly(PADPA)-Tvl-AOT was measured in the same way as described previously,[19] and it was found to be 4.3×10^{-5} S/cm, in the same range as the conductivity of PANI-TvL-AOT (6.6×10^{-5} S/cm)[19] and PANI-HRPC-AOT (3.2×10^{-5} S/cm).[19]

The XRD measurements of poly(PADPA)-TvL-AOT are shown in Figure 11 (as measured with Mo X-ray) and SI,

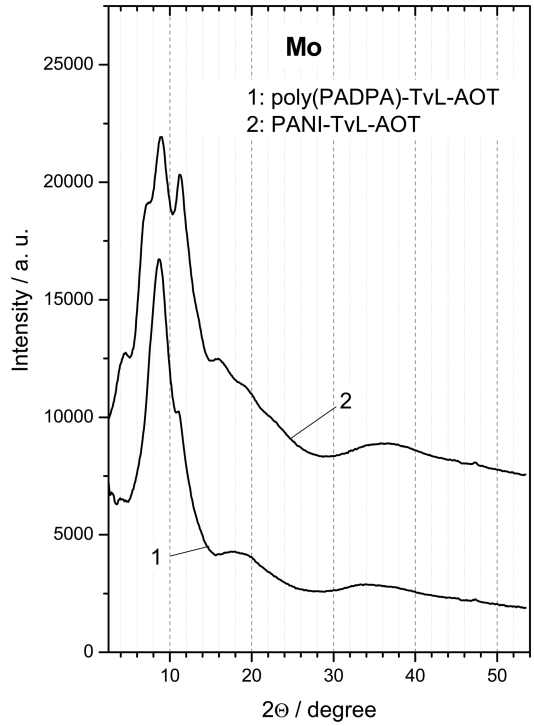

Figure 11. XRD powder diffraction spectra of poly(PADPA)-TvL-AOT (curve 1) and PANI-TvL-AOT (curve 2),[19] as measured with Mo X-ray.

Figure S11 (calculated for Cu X-ray). For comparison, the XRD pattern for PANI-TvL-AOT determined previously[19] is also given. In both records, there is one outstanding peak at $2\theta_{Mo}$ = 9°. The broadness of this peak and of the other peaks of minor intensity indicate that poly(PADPA)-TvL-AOT isolated from the reaction mixture was amorphous, similarly to PANI-TvL-AOT. The XRD pattern of poly(PADPA)-TvL-AOT is rather similar to the one of PANI-HRPC-AOT, see Junker et al.[19]

DISCUSSION

General Observations. The polymerization of PADPA with TvL/O_2 in the presence of AOT vesicles under optimal conditions—1.5 mM AOT, 1.0 mM PADPA, ≈ 32 nM TvL, pH = 3.5 (0.1 M H_3PO4 + NaH_2PO_4)—yields reaction products with more than 95% conversion that resemble PANI-ES if the UV/vis/NIR spectrum of the obtained poly(PADPA)-vesicle suspension (Figure 3) is compared with the spectrum of PANI-ES obtained with HRPC/H_2O_2.[15,16,31] In both cases, there is a strong absorption in the NIR region of the spectrum, with maximal intensity at about 1000 nm. For both products,

dx.doi.org/10.1021/cs500769d | ACS Catal. 2014, 4, 3421−3434

EPR measurements indicate the presence of unpaired electrons (Figure 5, Figure 10, and Junker et al.[15]). During the polymerization reaction, the EPR signal intensity increases with time and correlates with the increase in absorbance at λ = 1000 nm, see Figure 4B and Figure 5 for the formation of poly(PADPA) with TvL/O_2, and see Junker et al.[15] for the formation of PANI-ES with HRPC/H_2O_2. Despite these spectroscopic similarities, the poly(PADPA) prepared in this work, with TvL/O_2 in the presence of AOT vesicles at pH = 3.5, differs from PANI-ES obtained with HRPC/H_2O_2 in the presence of the same type of vesicles at pH = 4.3, see below. Moreover, there are clear differences between the poly(PADPA) obtained with TvL/O_2 and PANI obtained from aniline with TvL/O_2,[19] even if both reactions are carried out at the same pH = 3.5 and in the presence of the same AOT vesicles. The UV/vis/NIR spectrum of PANI obtained from aniline with TvL/O_2 indicates the formation of overoxidized products which may be due to the long time which is needed to complete the reaction for aniline,[19] whereas the oxidation and polymerization of PADPA is considerably faster (Figure 4) and much less TvL is required: ≈0.032 μM TvL for the polymerization of 1.0 mM PADPA versus ≈2.4 μM TvL to polymerize 2.0 mM aniline. If more TvL was used, overoxidized products were obtained (SI, Figure S6). For comparison, the polymerization of 4.0 mM aniline with HRPC/H_2O_2 was optimal at 0.92 μM HRPC concentration.[15]

MD Simulations. There is no doubt that the presence of the negatively charged AOT vesicles is essential for obtaining poly(PADPA) with the desired spectroscopic properties (see Figure 3 and Figure 5, and SI, Figures S7−S9). How the vesicles control the outcome of the reaction as a kind of template is, however, still not clear. It seems that a certain preorganization of the PADPA monomers in the region of the AOT bilayers before the oxidation and polymerization reactions are initiated is essential, although it is not clear which type of preorganization this could be. One approach we considered worth pursuing toward understanding molecular details of the vesicle template effect is to conduct MD simulations for better understanding the possible orientation of PADPA in the region of the AOT bilayer. In a first step, MD calculations of an AOT bilayer fragment alone (i.e. without added PADPA) were performed by simulating the conditions which correspond to the optimal reaction conditions with $[H_3PO_4] + [H_2PO_4^- Na^+]$ = 0.1 M and pH = 3.5 (SI, Figure S5). The AOT bilayer has a rather rough surface and becomes unstable if the simulation is made in absence of phosphate salt, which is in good agreement with experimental observations (no AOT vesicle formation in deionized water).[31] Simulations of an AOT bilayer fragment in the presence of phosphate salt (pH = 3.5) indicate that there is no specific perpendicular orientation of PADPA on the vesicle surface before oxidation is initiated. PADPA is partially inserted into the AOT bilayer, the orientation distribution of PADPA being centered at tilt angles of about 40 or 140° with respect to the bilayer normal (Figure 2C). A predominantly perpendicular preorientation of PADPA on the AOT vesicle surface before PADPA oxidation and polymerization is initiated by TvL/O_2 is therefore unlikely.

FTIR Measurements. The FTIR spectrum of the isolated poly(PADPA)-TvL-AOT shown in Figure 9 is very similar, but clearly not identical, to the PANI-ES spectra we recorded previously of samples obtained with HRPC/H_2O_2 from aniline in the presence of AOT vesicles, PANI-HRPC-AOT.[15] The spectrum in Figure 9 is also different from the FTIR spectra of the overoxidized PANI products obtained with TvL/O_2 from aniline, PANI-TvL-AOT.[19] Obviously, poly(PADPA) is a polymer different from PANI. There are notable differences, for example, in the relative band intensities at 748 and 879 cm^{-1}, both being stronger in the spectrum of poly(PADPA)-TvL-AOT. This may indicate that the poly(PADPA) chains obtained with TvL/O_2 are shorter than PANI chains obtained from aniline with HRPC/H_2O_2 or TvL/O_2, or that poly(PADPA)-TvL-AOT contains more 1,2-di- and/or 1,3,4-trisubstituted benzene rings than PANI-HRPC-AOT.

The FTIR spectrum of poly(PADPA)-TvL-AOT (Figure 9) is similar to the FTIR spectrum of a poly(PADPA) sample obtained with a purified *Trametes hirsuta* laccase at pH = 3.8 in the presence of sodium dodecylbenzenesulfonate micelles.[24] The major differences are the relative intensities of the characteristic bands between ≈1500 and 1600 cm^{-1}, and of the band at 879 cm^{-1}. This latter band is very weak (or even absent) in the spectrum of poly(PADPA) obtained in the micellar system,[24] possibly indicating that the product has shorter chains or contains more unwanted 1,2-disubstituted rings (Table 1). The most intense band at 1156 cm^{-1} (Figure 9) indicates presence of Q═NH^+-B or B-$NH^{\bullet+}$-B units (Table 1).

On the basis of a comparison of the FTIR spectrum of poly(PADPA)-TvL-AOT (Figure 9) with the FTIR spectrum of poly(PADPA) obtained by chemical oxidation with ammonium peroxydisulfate (APS) in 50 vol % ethanol, 50 vol % 0.2 M sulfuric acid under conditions, which yielded a PANI-ES-like product (APS/PADPA molar ratio = 1.5),[28] it seems that this chemically synthesized product and poly(PADPA)-TvL-AOT are very similar. The major poly(PADPA) bands for the enzymatically synthesized product (Figure 9) are located at 1572, 1506, and 1495 cm^{-1}, 1313, 1243, 1156, 879, 811, 750, and 696 cm^{-1}. For the chemically synthesized poly(PADPA),[28] the major bands are at 1574, 1506, and 1494 cm^{-1}, 1312, 1246, 1157, 874, 824, 750, and 693 cm^{-1}. A similar band like the one at 1672 cm^{-1} in the spectrum of the chemically synthesized poly(PADPA), assigned to oxygen-containing products,[28] could not be identified in poly(PADPA)-TvL-AOT because of occlusion by the strong carbonyl stretching vibration of AOT at 1734 cm^{-1} (Figure 9). Because the bands at 879 or 874 cm^{-1}, 750 cm^{-1}, and 696 or 693 cm^{-1} in the spectrum of the chemically synthesized poly(PADPA) can be assigned to tri- and monosubstituted aromatic amines[19] (Table 1), poly(PADPA) seems to be a polymer with relatively low molar mass. Poly(PADPA) must be a product which is (i) composed of short chains with many terminal groups like monosubstituted aromatic amines and (ii) a polymer with undesired trisubstituted benzene rings, independent of whether poly(PADPA) is synthesized with TvL/O_2 and AOT vesicles or chemically with APS. Furthermore, we note that, in agreement with experimental data for electrochemically polymerized PADPA,[41] poly(PADPA) indeed appears to be of low molar mass, and it has been argued why a high molar mass polymer—typical for PANI—cannot be obtained from PADPA.[41] The experiments carried out in this work with TvL confirm this general observation, as it is the case for poly(PADPA) prepared with *Trametes hirsuta* laccase in the presence of micellar templates.[24]

EPR Analysis and Conductivity Measurements. The EPR analysis shown in Figure 10 confirms that poly(PADPA) is structurally different from PANI-TvL-AOT or PANI-HRPC-AOT. In poly(PADPA) there are more isolated units with

dx.doi.org/10.1021/cs500769d | ACS Catal. 2014, 4, 3421−3434

radical character than in the case of the PANI samples. For all samples, the measured conductivity was low, indicating that charge transport between chains in the solid samples is hindered, most likely due to the presence of the bulky AOT in the isolated products, as discussed previously.[19,32]

ESI-MS Analysis. ESI-MS measurements were mainly carried out in order to quantify the depletion of PADPA during the polymerization reaction by analyzing the relative amount of remaining PADPA (Figure 6). This analysis showed extensive conversion (≈ 99%) after only 4 h under our reaction conditions (Figure 6C). Interestingly, the samples from the reactions carried out without vesicles indicated the presence of oxygen-containing PADPA derivatives, see Figure 8B. It seems that the vesicle templates suppress the formation of such unwanted products. This will be investigated further in a follow-up study.

CONCLUSIONS

The polymerization of PADPA can be carried out very efficiently at room temperature with TvL/O_2 in the presence of AOT vesicles as templates. The poly(PADPA) obtained has similar properties as chemically synthesized poly(PADPA).[28] In agreement with literature, poly(PADPA) is found to be different from PANI, independently on whether it is obtained chemically, electrochemically or enzymatically, although there are spectroscopic similarities between the two polymers. With the enzymatic method we applied, poly(PADPA)-TvL-AOT and PANI-HRPC-AOT are similar, but poly(PADPA) seems to be a much shorter polymer with more defects in the polymer (oligomer) chain (indication of the presence of 1,2-di- and 1,2,4-trisubstituted rings). Quantitative values or good estimates for the average molar mass of poly(PADPA), as obtained with TvL/O_2 and AOT vesicles by using the method developed in this paper, still need to be determined. Also, more details about the reaction mechanism need to be clarified in a future study. Despite this, the experimental observations made are promising, because we have shown that stable aqueous poly(PADPA)-vesicle suspensions can be obtained with much fewer enzymes (TvL) than the PANI-vesicle suspensions we prepared with TvL or HRPC: ≈ 0.032 μM TvL for poly(PAPDA) versus 2.4 μM TvL or 0.46 μM HRPC for PANI, if comparison is made on the basis of the same number of aniline repeating units. Compared to chemically synthesized poly(PADPA), the advantage of the enzymatic method is the high colloidal stability of the obtained suspension. This certainly is an advantage for possible applications, for example, as an ink for use in inkjet printers.[19]

ASSOCIATED CONTENT

Supporting Information

Data on the ESI-MS analysis, on the MD simulations, on the reaction optimization, and on control measurements are provided. This material is available free of charge via the Internet at http://pubs.acs.org.

AUTHOR INFORMATION

Corresponding Author

*E-mail: peter.walde@mat.ethz.ch.

Author Contributions

The manuscript was written through contributions of all authors. All authors have given approval to the final version of the manuscript.

Notes

The authors declare no competing financial interest.

ACKNOWLEDGMENTS

We thank Dr. Thomas Weber and Dr. Stefan Busato, both from the Department of Materials at ETH, for the XRD and conductivity measurements, respectively. The financial support by the Swiss National Science Foundation (200020-130472) is highly appreciated.

REFERENCES

(1) *Biocatalysis in Polymer Chemistry*; Loos, K., Ed.; Wiley-VCH Verlag & Co. KGaA: Weinheim, 2011.
(2) Singh, A.; Kaplan, D. L. *Adv. Polym. Chem.* **2006**, *194*, 211−224.
(3) Walde, P.; Guo, Z. *Soft Matter* **2011**, *7*, 316−331.
(4) Hollmann, F.; Arends, I. W. C. E. *Polymers* **2012**, *4*, 759−793.
(5) Sigg, S. J.; Seidi, F.; Renggli, K.; Silva, T. B.; Kali, G.; Bruns, N. *Macromol. Rapid Commun.* **2011**, *32*, 1710−1715.
(6) Kobayashi, S.; Makino, A. *Chem. Rev.* **2009**, *109*, 5288−5353.
(7) Gross, R. A.; Kumar, A.; Kalra, B. *Chem. Rev.* **2001**, *101*, 2097−2124.
(8) Mann, P. J. G.; Saunders, B. C. *Proc. R. Soc. London, Ser. B* **1935**, *119*, 47−60.
(9) Akkara, J. A.; Senecal, K. J.; Kaplan, D. L. *J. Polym. Sci., Part A: Polym. Chem.* **1991**, *29*, 1561−1574.
(10) Liu, W.; Cholli, A. L.; Nagarajan, R.; Kumar, J.; Tripathy, S.; Bruno, F. F.; Samuelson, L. *J. Am. Chem. Soc.* **1999**, *121*, 11345−11355.
(11) Liu, W.; Kumar, J.; Tripathy, S.; Samuelson, L. A. *Langmuir* **2002**, *18*, 9696−9704.
(12) Xu, P.; Singh, A.; Kaplan, D. L. *Adv. Polym. Sci.* **2006**, *194*, 69−94.
(13) Caramyshev, A. V.; Evtushenko, E. G.; Ivanov, V. F.; Barceló, A. R.; Roig, M. G.; Shnyrov, V. L.; van Huystee, R. B.; Kurochkin, I. N.; Vorobiev, A. K.; Sakharov, I. Y. *Biomacromolecules* **2005**, *6*, 1360−1366.
(14) Guo, Z.; Rüegger, H.; Kissner, R.; Ishikawa, T.; Willeke, M.; Walde, P. *Langmuir* **2009**, *25*, 11390−11405.
(15) Junker, K.; Zandomeneghi, G.; Guo, Z.; Kissner, R.; Ishikawa, T.; Kohlbrecher, J.; Walde, R. *RSC Adv.* **2012**, *2*, 6478−6495.
(16) Junker, K.; Gitsov, I.; Quade, N.; Walde, P. *Chem. Pap.* **2013**, *67*, 1028−1047.
(17) Bouldin, R.; Kokil, A.; Ravichandran, S.; Nagarajan, S.; Kumar, J.; Samuelson, L. A.; Bruno, F. F.; Nagarajan, R. In *Green Polymer Chemistry: Biocatalysis and Biomaterials*, Cheng, H. N., Gross, R. A., Eds.; ACS Symposium Series: Washington, DC, 2010; Chapter 23, pp 315−341.
(18) Ochoteco, E.; Mecerreyes, D. *Adv. Polym. Sci.* **2010**, *237*, 1−19.
(19) Junker, K.; Kissner, R.; Rakvin, B.; Guo, Z.; Willeke, M.; Busato, S.; Weber, T.; Walde, P. *Enzyme Microb. Technol.* **2014**, *55*, 72−84.
(20) Jonsson, M.; Lind, J.; Eriksen, T. E.; Merényi, G. *J. Am. Chem. Soc.* **1994**, *116*, 1423−1427.
(21) Shleev, S. V.; Morozova, O. V.; Nikitina, O. V.; Gorshina, E. S.; Rusinova, T. V.; Serezhenkov, V. A.; Burbaev, D. S.; Gazaryan, I. G.; Yaropolov, A. I. *Biochimie* **2004**, *86*, 693−703.
(22) Xu, F. *J. Biol. Chem.* **1997**, *272*, 924−928.
(23) Gospodinova, N.; Terlemezyan, L. *Prog. Polym. Sci.* **1998**, *23*, 1443−1484.
(24) Shumakovich, G.; Streltsov, A.; Gorshina, E.; Rusinova, T.; Kurova, V.; Vasil'eva, I.; Otrokhov, G.; Morozova, O.; Yaropolov, A. *J. Mol. Catal. B: Enzym.* **2011**, *69*, 83−88.
(25) Bhadra, S.; Khastgir, D.; Singha, N. K.; Lee, J. H. *Prog. Polym. Sci.* **2009**, *34*, 783−810.
(26) Wallace, G. G.; Spinks, G. M.; Kane-Maguire, L. A. P.; Teasdale, P. R. In *Conductive Electroactive Polymers: Intelligent Polymer Systems*, 3rd ed.; CRC Press, Taylor & Francis Group: Boca Raton, FL, 2009; Chapters 4 and 5.
(27) Ćirić-Marjanović, G. *Synth. Met.* **2013**, *177*, 1−47.

(28) Ćirić-Marjanović, G.; Trchová, M.; Konyushenko, E. N.; Holler, P.; Stejskal, J. *J. Phys. Chem. B* **2008**, *112*, 6976−6987.
(29) Bertrand, T.; Jolivalt, C.; Briozzo, P.; Caminade, E.; Joly, N.; Madzak, C.; Mougin, C. *Biochemistry* **2002**, *41*, 7325−7333.
(30) Piontek, K.; Antorini, M.; Choinowski, T. *J. Biol. Chem.* **2002**, *277*, 37663−37669.
(31) Guo, Z.; Hauser, N.; Moreno, A.; Ishikawa, T.; Walde, P. *Soft Matter* **2011**, *7*, 180−193.
(32) Rakvin, B.; Carić, D.; Andreis, M.; Junker, K.; Walde, P. *J. Phys. Chem. B* **2014**, *118*, 2205−2213.
(33) Berendsen, H. J. C.; Postma, J. P. M.; van Gunsteren, W. F.; DiNola, A.; Haak, J. R. *J. Chem. Phys.* **1984**, *81*, 3684−3690.
(34) Horta, B. A. C.; Hünenberger, P. H. *J. Am. Chem. Soc.* **2011**, *133*, 8464−8466.
(35) Grillo, I.; Kats, E. I.; Muratov, A. R. *Langmuir* **2003**, *19*, 4573−4581.
(36) Berendsen, H. J. C.; Potsma, J. P. M.; van Gunsteren, W. F.; Hermans, J. In *Intermolecular Forces*; Pullman, B., Ed.; Reidel: Dordecht, The Netherlands, 1981; pp 331−342.
(37) Malval, J. P.; Morand, J. P.; Lapouyade, R.; Rettig, W.; Jonusauskas, G.; Oberlé, A.; Trieflinger, C.; Daub, J. *Photochem. Photobiol. Sci.* **2004**, *3*, 939−948.
(38) Xia, Y.; Wiesinger, J. M.; Mac Diarmid, A. G.; Epstein, A. J. *Chem. Mater.* **1995**, *7*, 443−445.
(39) Kulikov, A. V.; Komissarova, A. S.; Shestakov, A. F.; Fokeeva, L. S. *Russ. Chem. Bull.* **2007**, *56*, 2026−2033.
(40) Santana, V. T.; Nascimento, O. R.; Djurado, D.; Travers, J. P.; Pron, A.; Walmsley, L. *J. Phys.: Condens. Matter* **2013**, *25*, 116004 (6 pages).
(41) Kitani, A.; Yano, J.; Kunai, A.; Sasaki, K. *J. Electroanal. Chem.* **1987**, *221*, 69−82.
(42) Dmitrieva, E.; Dunsch, L. *J. Phys. Chem. B* **2011**, *115*, 6401−6411.
(43) Geniès, E. M.; Penneau, J. F.; Lapkowski, M.; Boyle, A. *J. Electroanal. Chem.* **1989**, *269*, 63−75.
(44) Ding, Y.; Padias, A. B.; Hall, H. K., Jr. *J. Polym. Chem.* **1999**, *37*, 2569−2579.
(45) Jonsson, M.; Pettersson, E.; Reinhammar, B. *Acta Chem. Scand.* **1968**, *22*, 2135−2140.
(46) Trchová, M.; Stejskal, J. *Pure Appl. Chem.* **2011**, *83*, 1803−1817.

NOTE ADDED AFTER ASAP PUBLICATION

After this paper was published ASAP on September 2, 2014, a correction was made to the footnote of Scheme 2. The corrected version was reposted September 3, 2014.